ANIMAL CELLS AND SYSTEMS
2020, VOL. 24, NO. 2, 91–98
https://doi.org/10.1080/19768354.2020.1752306

Taylor & Francis
Taylor & Francis Group

Generation of embryonic stem cells derived from the inner cell mass of blastocysts of outbred ICR mice

Na Rae Han [a], Song Baek [a], Hwa-Young Kim[a], Kwon Young Lee[b], Jung Im Yun [c], Jung Hoon Choi[b], Eunsong Lee [b], Choon-Keun Park[a,d] and Seung Tae Lee [a,d,e]

[a]Department of Animal Life Science, Kangwon National University, Chuncheon, Korea; [b]College of Veterinary Medicine and Institute of Veterinary Science, Kangwon National University, Chuncheon, Korea; [c]Institute of Animal Resources, Kangwon National University, Chuncheon, Korea; [d]Department of Applied Animal Science, Kangwon National University, Chuncheon, Korea; [e]KustoGen Inc., Chuncheon, Korea

ABSTRACT

Embryonic stem cells (ESCs) derived from outbred mice which share several genetic characteristics similar to humans have been requested for developing stem cell-based bioengineering techniques directly applicable to humans. Here, we report the generation of ESCs derived from the inner cell mass of blastocysts retrieved from 9-week-old female outbred ICR mice mated with 9-week-old male outbred ICR mice ($_{ICR}$ESCs). Similar to those from 129/Ola mouse blastocysts ($_{E14}$ESCs), the established $_{ICR}$ESCs showed inherent characteristics of ESCs except for partial and weak protein expression and activity of alkaline phosphatase. Moreover, $_{ICR}$ESCs were not originated from embryonic germ cells or pluripotent cells that may co-exist in outbred ICR strain-derived mouse embryonic fibroblasts ($_{ICR}$MEFs) used for deriving colonies from inner cell mass of outbred ICR mouse blastocysts. Furthermore, instead of outbred $_{ICR}$MEFs, hybrid $_{B6CBAF1}$MEFs as feeder cells could sufficiently support *in vitro* maintenance of $_{ICR}$ESC self-renewal. Additionally, $_{ICR}$ESC-specific characteristics (self-renewal, pluripotency, and chromosomal normality) were observed in $_{ICR}$ESCs cultured for 40th subpassages (164 days) on $_{B6CBAF1}$MEFs without any alterations. These results confirmed the successful establishment of ESCs derived from outbred ICR mice, and indicated that self-renewal and pluripotency of the established $_{ICR}$ESCs could be maintained on $_{B6CBAF1}$MEFs in culture.

ARTICLE HISTORY
Received 30 December 2019
Revised 3 March 2020
Accepted 18 March 2020

KEYWORDS
Embryonic stem cells; outbred; ICR; establishment; B6CBAF1 strain-derived mouse embryonic fibroblasts

DEVELOPMENTAL BIOLOGY

Introduction

Embryonic stem cells (ESCs) with self-renewal and pluripotency properties have attracted a great deal of interest as a model of organogenesis during embryogenesis in developmental biology (Dvash et al. 2006; Prajumwongs et al. 2016) and as a source of cells for cell therapies in regenerative medicine (Trounson and McDonald 2015; Duncan and Valenzuela 2017). Furthermore, they have been used for the generation of genetically modified animals, screening of drugs without clinical experiments, and for the development of personalized drug treatment regimens (Kawamata and Ochiya 2010; Lou and Liang 2011; Lee et al. 2020). Therefore, they have been actively applied not only in basic research in the fields of regenerative medicine, transgenic animal research, and pharmaceutics (Prajumwongs et al. 2016; Ukai et al. 2017), but also in clinical research (Ilic et al. 2015; Duncan and Valenzuela 2017).

In the early stages of stem cell research, ESCs derived from blastocysts of mice with a variety of genetic backgrounds were widely used for the development of stem cell-related techniques (Arufe et al. 2006; Ouyang et al. 2007). Commencing with generation of the first mouse ESCs derived from the 129SvE strain in 1981 (Evans and Kaufman 1981; Martin 1981), attempts have been made to establish mouse ESCs (mESCs) derived from a variety of strains (Schoonjans et al. 2003; Tanimoto et al. 2008; Nichols and Smith 2011). However, successful establishment of mESC lines have been limited to a few permissive strains, such as 129 and C57BL/6 sub-strains (Tanimoto et al. 2008; Nichols and Smith 2011). Simultaneously, the generation of mESCs derived from non-permissive strains that are refractory to ESC generation, such as ICR, CBA, NOD, DBA, and BALB/c, showed extremely low efficiency (Kawase et al. 1994).

CONTACT Seung Tae Lee stlee76@kangwon.ac.kr Department of Animal Life Science, Kangwon National University, Chuncheon 24341, Korea; Department of Applied Animal Science, Kangwon National University, Chuncheon 24341, Korea; KustoGen Inc., Chuncheon 24341, Korea
Supplemental data for this article can be accessed at https://doi.org/10.1080/19768354.2020.1752306.

As the genetic identity between mice and humans is approximately 99%, various laboratory mouse strains, including inbred, hybrid, and outbred mice, have been widely used for research purposes (Fox et al. 2006). Consistent results can be obtained from inbred mice with good genetic and phenotypic stability (Yoshiki and Moriwaki 2006; Choi et al. 2017), whereas the impaired homeostasis regulation-related genes are trouble in recovery because of their genetic homology at chromosomes (Fox et al. 2006). Hybrid mice generated by deliberately crossing mice of two inbred strains maintain genetic and phenotypic uniformity, similar to inbred stains (National Research Council 1999). However, acquisition of data related to genetic background may be difficult (Schauwecker 2011). On the other hand, outbred mice have genetic characteristics similar to humans, including undefined genetics and phenotypic variation, and a high degree of heterogeneity (Chia et al. 2005; Jensen et al. 2016). They have also been shown to be useful as base populations for selection in producing new or improved humanized mouse models (Zuluaga et al. 2006). The results obtained from outbred stocks are generally considered more valuable than those from inbred or hybrid strains for application of the results to humans (Shin et al. 2017). Therefore, toxicology, pharmacology, and fundamental biomedical research continue to be performed using outbred mice (Chia et al. 2005).

To date, there have been a few reports regarding the establishment of ESC lines derived from outbred ICR mouse blastocysts (Meng et al. 2003; Lee et al. 2012). These establishment of ESC lines derived from denuded intact embryos or blastomeres of ICR mice was mainly conducted under microenvironments specialized by the addition of diverse extrinsic factors such as knockout serum replacement (KSR), differentiation inhibitors and proliferation stimulators as an alternative for enhancing derivation efficiency (Lee et al. 2012). However, any characterization and long-term culture of the established ICR mice-derived ESCs have not been reported (Lee et al. 2012). In addition, the usage of extrinsic factors in the establishment of ESCs resulted in reduction of ESC viability (Naujok et al. 2014) and alteration of ESC characteristics (Wu et al. 2015). Therefore, with establishment of ESC lines derived from outbred ICR mice under extrinsic factors-free microenvironments, their characterization and long-term culture system development should be required for enhancing their usability.

Here, we report the establishment of ESC lines derived from outbred stocks of ICR mice. ICR stock mESCs were isolated and cultured *in vitro* from the inner cell mass of blastocysts derived from outbred ICR mice, and their identity was confirmed based on parameters related to self-renewal and differentiation potential.

Materials and methods

Detailed information of all experimental procedures and statistical analysis performed in this study can be found in the supplementary information.

Results

Establishment of $_{ICR}$ESCs

Establishment of $_{ICR}$ESCs was performed according to the procedure presented in Figure 1. Of the 218 blastocysts produced from outbred ICR mice, 115 blastocysts were adherent to $_{ICR}$MEF feeder cells and 106 colonies grew out from the inner cell masses of the 115 $_{ICR}$MEF-adherent blastocysts. However, in establishing ESCs from 106 outgrown colonies, only one ESC was successfully maintained over the 14th subpassage. Subsequently, the established $_{ICR}$ESCs were characterized between the 15th and 20th subpassages. Similar to $_{E14}$ESC colonies (upper right in Figure 2(A)), colonies of $_{ICR}$ESCs showed well-defined boundaries and dome-shaped morphology (Figure 2(A)). AP protein expression (Figure 2(B)) and activity (Figure 2(C)) were observed partially and weakly in a portion of $_{ICR}$ESC colonies, unlike $_{E14}$ESCs showing strong AP protein expression (upper right in Figure 2(B)) and activity (upper right in Figure 2(C)) throughout the colonies. Additionally, the established $_{ICR}$ESCs showed the same expression pattern as $_{E14}$ESCs with regard to the transcription and translation of self-renewal-related genes. With the successful transcriptional expression of *Oct4*, *Sox2*, *Nanog*, *Tert*, and *AP* (Figure 2(D)), positive expression of Oct4 (Figure 2(E)), Sox2 (Figure 2(F)), and Nanog (Figure 2(G)), and negative expression of Tra-1-60 (Figure 2(H)) and Tra-1-81 (Figure 2(I)) were detected in both the established $_{ICR}$ESCs (Figure 2(E–I)) and the $_{E14}$ESCs (upper right in Figure 2 (E–I)). In addition, the EBs formed from $_{ICR}$ESCs (Figure 2(J)) showed lineage-specific differentiation into endoderm, mesoderm, and ectoderm. The spontaneously differentiated EBs showed positive staining for neurofilaments as an ectodermal marker (Figure 2(K)), α-smooth muscle actin as a mesodermal marker (Figure 2(L)), and cytokeratin 18 as an endodermal marker (Figure 2(M)). The teratomas formed from $_{ICR}$ESCs transplanted into nude mice included ducts with simple columnar epithelial cells (endodermal lineage; Figure 2(N1)), blood vessels (endodermal lineage; Figure 2(N2)), simple cuboidal cells (endodermal lineage; Figure 2(N3)), chondrocyte

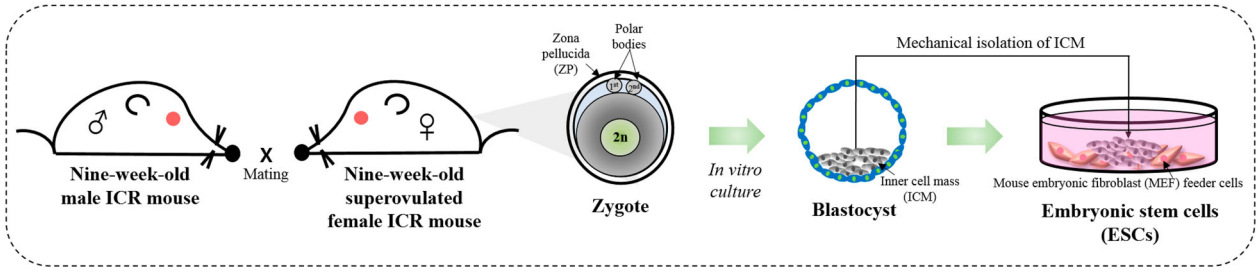

Figure 1. Schematic diagram depicting the procedure to establish embryonic stem cells (ESCs) from outbred ICR mice blastocysts ($_{ICR}$-ESCs). Nine-week-old female ICR mice superovulated by injection with pregnant mare serum gonadotropin and human chorionic gonadotropin were mated with nine-week-old male ICR mice. Next, zygotes with a 2nd polar body and pronucleus were obtained from oviduct of female ICR mice and *in-vitro*-cultured for inducing generation of blastocysts. Subsequently, inner cell mass was retrieved from collected blastocysts and cultured on mitotically inactivated mouse embryonic fibroblasts (MEFs) feeder cells derived from fetuses of outbred ICR mice ($_{ICR}$MEFs) for generation of $_{ICR}$ESCs.

(mesodermal lineage; Figure 2(N4)), adipocytes (mesodermal lineage; Figure 2(N5)), muscle cells (mesodermal lineage; Figure 2(N6)), neural tubes (ectodermal lineage; Figure 2(N7)), germinal hair bulb-like structures with pigmented cells in the core region (ectodermal lineage; Figure 2(N8)), and nervous tissue (ectodermal lineage; Figure 2(N9)). Differentiation of $_{ICR}$ESCs into germ cells induced successful generation of oocyte-like cells with ZP (Figure 2(O), arrowhead). The established $_{ICR}$ESCs had a normal diploid karyotype of 40 (Figure 2(P)) and their sex was confirmed as female by identifying the presence of X-chromosome-specific *Xist* and the absence of Y-chromosome-specific *Zfy1* in the genome (Figure 2(Q)). Subsequently, to determine whether $_{ICR}$ESCs originated from embryonic germ cells or pluripotent cells that may co-exist in $_{ICR}$MEF feeder cells, $_{ICR}$MEF feeder cells used in the process of ESC establishment were cultured for 14 days in standard ESC culture medium. Throughout the culture period, no dome-shaped colonies were formed on the cultured $_{ICR}$MEF feeder cells (Supplementary Figure S1A) and the yield of cells positive for pluripotent stem cell-specific proteins (Oct4, Sox2, and Nanog) and embryonic germ cell-specific protein (VASA) was extremely low (< 1%) in the cultured $_{ICR}$MEFs (Supplementary Figure S1B), indicating that the established $_{ICR}$ESCs were not derived from pluripotent stem cells or embryonic germ cells in the $_{ICR}$MEF feeder cell population. These results confirmed that the $_{ICR}$ESCs with self-renewal ability and pluripotency could be successfully established from the inner cell mass of blastocysts derived from outbred ICR mice.

Establishment of MEF feeder cell-based culture system customized to $_{ICR}$ESCs

Subsequently, the strain of MEF feeder cells sufficiently supporting the *in vitro* maintenance of $_{ICR}$ESC self-renewal was determined by analyzing the doubling time, colony size, and number, and self-renewal-related protein expression among $_{ICR}$ESCs cultured on MEF feeder cells derived from outbred ICR, inbred C57BL/6, and hybrid B6CBAF1 mice. The results indicated that $_{ICR}$ESCs maintained on $_{C57BL/6}$MEFs showed significantly longer doubling time (Supplementary Figure S2A), smaller colony size (Supplementary Figure S2B), and fewer colonies (Supplementary Figure S2C) than those on $_{ICR}$MEFs and $_{B6CBAF1}$MEFs, which did not differ significantly from each other in each of the above parameters. Moreover, there were no significant differences in expression of self-renewal-related proteins (Oct4, Sox2, and Nanog) among $_{ICR}$ESCs cultured on $_{ICR}$MEFs, $_{C57BL/6}$MEFs, and $_{B6CBAF1}$MEFs (Supplementary Figure S2D). These results indicated that MEF feeder cells derived from ICR and B6CBAF1 mice were useful for maintaining the self-renewal of ESCs derived from ICR mice. Furthermore, as the genetic background of feeder cells used for *in vitro* culture should be different from the cultured ESCs for eliminating cellular contamination derived from feeder cells, we confirmed that the usage of MEF feeder cells derived from B6CBAF1 mice in the *in vitro* culture of $_{ICR}$ESCs was the best choice for maintenance of their self-renewal capability. Subsequently, culture of $_{ICR}$ESCs was conducted on hybrid $_{B6CBAF1}$MEFs from the 21st subpassage.

Characterization of long-term cultured $_{ICR}$ESCs in the $_{ICR}$ESC-optimized MEF feeder cell-based culture system

To examine the usefulness of the $_{ICR}$ESC-optimized MEF feeder cell-based culture system for long-term maintenance of $_{ICR}$ESCs, the $_{ICR}$ESCs at the 21st subpassage were cultured on hybrid $_{B6CBAF1}$MEFs until the 34th subpassage and long-term cultured $_{ICR}$ESCs were characterized

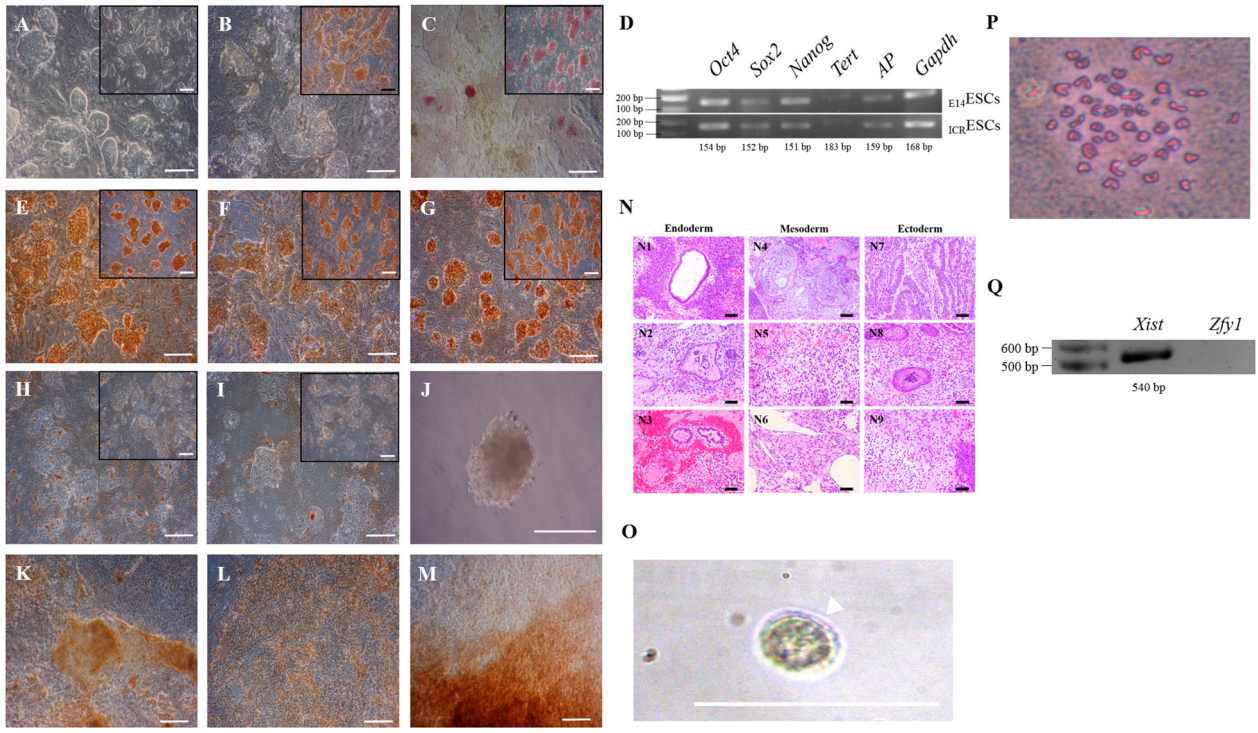

Figure 2. Characterization of embryonic stem cells established from outbred ICR mice blastocysts. The $_{ICR}$ESCs were established and maintained on mitotically inactivated MEFs derived from ICR mice and cell subpassage was conducted every 4 days. Moreover, characterization of $_{ICR}$ESCs was performed between passages 15 and 20. (A) Colony morphology of $_{ICR}$ESCs ($n = 3$). Dome-shaped morphology of $_{ICR}$ESC colonies was maintained during culture, similar to $_{E14}$ESC colonies (upper right in A). Scale bar, 200 µm. (B and C) Alkaline phosphatase (AP) protein expression and activity ($n = 3$). Both AP protein expression (B) and activity (C) were identified partially in the colonies of $_{ICR}$ESCs, whereas the colonies of $_{E14}$ESCs showed strong AP protein expression (upper right in B) and activity (upper right in C). Scale bar, 200 µm. (D) Transcriptional expression of self-renewal-related genes ($n = 3$). Transcripts of self-renewal-related genes, *Oct4*, *Sox2*, *Nanog*, *Tert*, and *AP*, were detected in $_{ICR}$ESCs, similar to $_{E14}$ESCs. (E–I) Translational expression of self-renewal-related genes ($n = 3$). Like $_{E14}$ESCs (upper right in E–I), $_{ICR}$ESCs showed positive staining for Oct4, Sox2, and Nanog and negative staining for Tra-1-60 and Tra-1-81. Scale bar, 200 µm. (J) Embryoid body (EB) formation ($n = 3$). $_{ICR}$ESCs were cultured for 3 days in feeder- and leukemia inhibitory factor (LIF)-free environment to allow differentiation into EBs, and EBs with spherical morphology were observed. Scale bar, 200 µm. (K–M) Spontaneous *in vitro* differentiation into three germ layers ($n = 3$). EBs were differentiated further by culturing for 7 days without feeder cells and LIF, and cells derived from the differentiated EBs showed immunoreactivity for neurofilaments (ectoderm; K), α-smooth muscle actin (mesoderm; L), and cytokeratin 18 (endoderm; M). Scale bar, 200 µm. (N) *In vivo* differentiation into three germ layers ($n = 3$). Transplantation of $_{ICR}$ESCs into nude mice showed successful teratoma formation at 5 weeks. Teratoma stained with hematoxylin and eosin contained endoderm (ducts with simple columnar epithelial cells, blood vessels, and simple cuboidal cells), mesoderm (chondrocytes, adipocytes, and muscle cells), and ectoderm (neural tubes, germinal hair bulb-like structure with pigmented cells in the core region, and nervous tissue). Scale bar, 50 µm. (O) Differentiation into oocytes ($n = 3$). Oocyte-like cells with zona pellucida (arrowhead) were derived from large-sized germ cells differentiated from the $_{ICR}$ESCs. Scale bar, 50 µm. (P) Karyotyping ($n = 3$). A normal diploid karyotype of 40 was identified in the established $_{ICR}$ESCs. (Q) Sex determination ($n = 3$). Sexing was performed by checking for the presence of X-chromosome-specific *Xist* or Y-chromosome-specific *Zfy1* in the genome. *Xist* and *Zfy1* were present and absent in the genome of $_{ICR}$ESCs, respectively, indicating that they were female.

between the 35th and 40th subpassages. All colonies derived from $_{E14}$ESCs (upper right in Figure 3(A)) and $_{ICR}$ESCs (Figure 3(A)) had well-defined boundaries and dome-shaped morphology. Strong AP protein expression (upper right in Figure 3(B)) and activity (upper right in Figure 3(C)) were detected throughout all colonies derived from $_{E14}$ESCs, whereas a portion of the colonies derived from $_{ICR}$ESCs showed partial and weak AP protein expression (Figure 3(B)) and activity (Figure 3 (C)). Moreover, no significant differences were observed in *Oct4*, *Sox2*, *Nanog*, *Tert*, and *AP* expression at the transcriptional level in $_{ICR}$ESCs cultured for a long time on $_{B6CBAF1}$MEFs compared to $_{ICR}$ESCs at an early subpassage (Figure 3(D)). The long-term cultured $_{ICR}$ESCs (Figure 3(E–I)) showed an equivalent expression pattern to $_{E14}$ESCs with regard to Oct4, Sox2, Nanog, Tra-1-60, and Tra-1-81 (upper right in Figure 3(E–I)) as follows: positive for Oct4 (Figure 3(E)), Sox2 (Figure 3(F)), and Nanog (Figure 3(G)), and negative for Tra-1-60 (Figure 3(H)) and Tra-1-81 (Figure 3(I)). With successful formation of EBs from long-term cultured $_{ICR}$ESCs (Figure 3(J)), neurofilaments as an ectodermal marker (Figure 3(K)), α-smooth

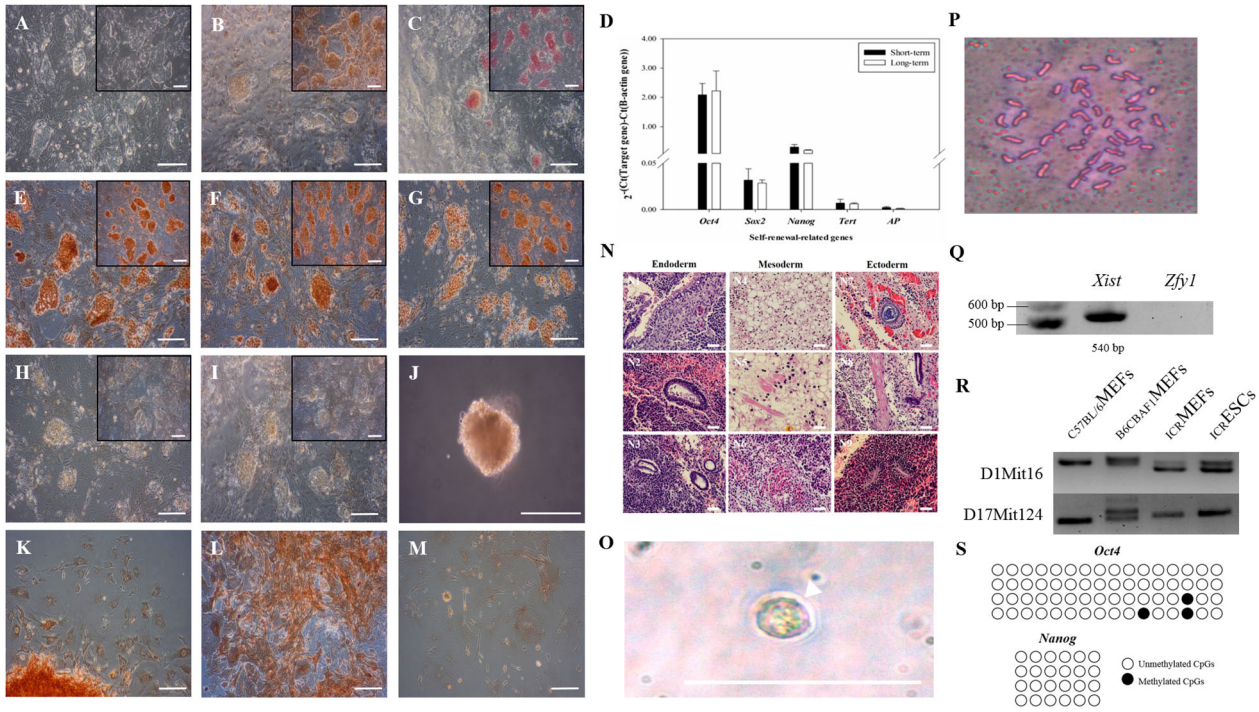

Figure 3. Characterization of long-term cultured $_{ICR}$ESCs on $_{B6CBAF1}$MEFs. The $_{ICR}$ESCs at the 20th subpassage were cultured on mitotically inactivated $_{B6CBAF1}$MEFs and subpassaged at intervals of 4 days. Subsequently, characterization of the cultured $_{ICR}$ESCs was performed at passages between 35 and 40. (A) Colony morphology of $_{ICR}$ESCs ($n = 3$). The $_{ICR}$ESCs showed a dome-shaped morphology, similar to $_{E14}$ESCs (upper right in A). Scale bar, 200 µm. (B and C) AP protein expression and activity ($n = 3$). Partial weak AP protein expression (B) and activity (C) were detected in the colonies of $_{ICR}$ESCs, whereas strong AP protein expression (upper right in B) and activity (upper right in C) were identified in the $_{E14}$ESCs. Scale bar, 200 µm. (D) Transcriptional expression of self-renewal-related genes ($n = 3$). Levels of *Oct4*, *Sox2*, *Nanog*, *Tert*, and *AP* transcripts in long-term (above 35th subpassage) cultured $_{ICR}$ESCs were not significantly different from those in short-term (below 20th subpassage) cultured $_{ICR}$ESCs. (E–I) Translational expression of self-renewal-related genes ($n = 3$). The $_{ICR}$ESCs stained positively for Oct4, Sox2, and Nanog and negatively for Tra-1-60 and Tra-1-81, similar to $_{E14}$ESCs (upper right in E–I). Scale bar, 200 µm. (J) Embryoid body (EB) formation ($n = 3$). EBs with spherical colony morphology were successfully generated in feeder- and LIF-free environment for 3 days. Scale bar, 200 µm. (K–M) Spontaneous *in vitro* differentiation into three germ layers ($n = 3$). EBs were differentiated for 7 days in feeder- and LIF-free environment and cells differentiated from EBs showed immunoreactivity to neurofilaments (ectoderm; K), α-smooth muscle actin (mesoderm; L), and cytokeratin 18 (endoderm; M). Scale bar, 200 µm. (N) *In vivo* differentiation into three germ layers ($n = 3$). Transplantation of $_{ICR}$ESCs into nude mice showed successful teratoma formation at 5 weeks. Staining of the teratomas with hematoxylin and eosin showed endodermal (gut epithelium, double-layered apocrine ducts, and ducts consisting of simple cuboidal cells), mesodermal (adipocytes, striated muscle, and smooth muscle cells), and ectodermal (epithelium with keratinization, nerve bundles, and neural epithelium) tissues. Scale bar, 50 µm. (O) Differentiation into oocytes ($n = 3$). Oocyte-like cells with zona pellucida (arrowhead) were derived from large-sized germ cells differentiated from the $_{ICR}$ESCs. Scale bar, 50 µm. (P) Karyotyping ($n = 3$). The long-term cultured $_{ICR}$ESCs showed a normal diploid karyotype of 40. (Q) Sex determination ($n = 3$). *Xist* was present and *Zfy1* was absent in the genome of the long-term cultured $_{ICR}$ESCs, indicating that they were female. (R) Analysis of microsatellite DNA ($n = 3$). Alleles of D1Mit16 and D17Mit124 markers were identical between $_{ICR}$MEFs and $_{ICR}$ESCs. By contrast, alleles of D1Mit16 and D17Mit124 markers in $_{ICR}$ESCs were different from those of $_{C57BL/6}$MEFs and $_{B6CBAF1}$MEFs. (S) Methylation analysis of *Oct4* and *Nanog* promoter regions. Open and filled circles represent unmethylated and methylated CpGs, respectively. The status of *Oct4* and *Nanog* promoter regions in $_{ICR}$ESCs was largely unmethylated.

muscle actin as a mesodermal marker (Figure 3(L)), and cytokeratin 18 as an endodermal marker (Figure 3(M)) were detected in spontaneously differentiated EBs. Additionally, following transplantation into nude mice, the long-term cultured $_{ICR}$ESC-derived teratomas showed gut epithelium (endodermal lineage; Figure 3 (N1)), double-layered apocrine duct (endodermal lineage; Figure 3(N2)), ducts consisting of simple cuboidal cells (endodermal lineage; Figure 3(N3)), adipocytes (mesodermal lineage; Figure 3(N4)), striated muscle (mesodermal lineage; Figure 3(N5)), smooth muscle cells (mesodermal lineage; Figure 3(N6)), epithelium with keratinization (ectodermal lineage; Figure 3(N7)), nerve bundles (ectodermal lineage; Figure 3(N8)), and neural epithelium (ectodermal lineage; Figure 3(N9)). Differentiation of long-term cultured $_{ICR}$ESCs into germ cells induced successful generation of oocyte-like cells with ZP (Figure 3(O), arrowhead). The long-term cultured

$_{ICR}$ESCs showed a normal diploid karyotype of 40 (Figure 3(P)), and the presence of X-chromosome-specific *Xist* and the absence of Y-chromosome-specific *Zfy1* in their genome (Figure 3(Q)), indicating that their sex was female. Moreover, alleles detected in $_{ICR}$ESCs by the microsatellite markers D1Mit16 and D17Mit124 were equally observed in $_{ICR}$MEFs (Figure 3(R)), whereas alleles of $_{ICR}$ESCs were different from those of $_{C57BL/6}$MEFs and $_{B6CBAF1}$MEFs (Figure 3(R)). The hypomethylated status of *Oct4* and *Nanog* promoter regions were observed in the long-term cultured $_{ICR}$ESCs (Figure 3(S)), indicating that these gene promoters in $_{ICR}$ESCs are active and the $_{ICR}$ESCs retain pluripotency. These results clearly indicated that $_{ICR}$ESCs were derived from blastocysts of outbred ICR mice. Despite long-term culture of $_{ICR}$ESCs on $_{B6CBAF1}$MEFs, self-renewal, pluripotency, and chromosomal normality could be successfully maintained without any alterations, indicating that *in vitro* culture of $_{ICR}$ESCs on $_{B6CBAF1}$MEFs is a MEF feeder cell-based culture system customized to established $_{ICR}$ESCs.

Discussion

In this study, $_{ICR}$ESCs were successfully derived from one of 218 blastocysts retrieved from outbred ICR mice. Unusually, weak AP protein expression and activity were observed in the derived $_{ICR}$ESCs. Nevertheless, the derived $_{ICR}$ESCs had a normal female karyotype and showed characteristics of stem cells: colonies with well-defined boundaries and dome-shaped morphology, transcriptional and translational expression of self-renewal-related genes, *in vitro* and *in vivo* differentiation into three germ layers, and germ cell differentiation. Moreover, $_{ICR}$ESCs maintained for a long time on $_{B6CBAF1}$-MEFs showed no loss of stem cell-related characteristics and no abnormalities of female karyotype. Therefore, we established ESCs derived from blastocysts of outbred ICR mice and developed a system for culture of $_{ICR}$ESCs using $_{B6CBAF1}$MEFs. A pathway for deriving more human-similar results in a mouse model could be developed.

In addition to Oct4, Sox2, and Nanog, AP is conventionally used as an ESC-specific marker regardless of species (Tielens et al. 2006). Interestingly, as shown in Figures 2(B,C) and 3(B,C), weak protein expression and activity of AP were detected in $_{ICR}$ESCs in comparison to $_{E14}$ESCs, which is a widely used ESC line. In previous studies, the regulation of tissue nonspecific AP was shown to be affected by p38 mitogen-activated protein kinase (MAPK) (Suzuki et al. 2002; Rey et al. 2007), and decreased protein level and activity were detected in p38$^{-/-}$ mouse ESCs with no changes in pluripotent marker expression (Štefková et al. 2015). Accordingly, it is possible that expression of p38 kinase in $_{ICR}$ESCs may be decreased more than other ESCs, resulting in weak protein expression and activity of AP. Subsequently, for verifying the hypothesis, we quantified expression of p38 MAPK proteins, and there was no significant difference in the amount of p38 MAPK proteins expressed in between the $_{E14}$ESCs and the $_{ICR}$ESCs (Supplementary Figure S3). These results demonstrate that weak protein expression and activity of AP in $_{ICR}$ESCs result from not expression of p38 MAPK proteins but another unknown factors. Of course, studies on the another unknown factors should be conducted in the future.

Although human ESCs differentiated into numerous types of cells are considered valuable tools for cell therapy (Gerecht-Nir and Itskovitz-Eldor 2004; Ryu et al. 2019), their maintenance and manipulation are costly and difficult, and require high-end facilities of good manufacturing practice (GMP) level (McKee and Chaudhry 2017; Ye et al. 2017). By contrast, maintenance and manipulation of the established $_{ICR}$ESCs are cheaper and easier than those of human ESCs and advanced facilities are not required. Additionally, the results derived from $_{ICR}$ESCs with similar genetic characteristics or heterogeneity to humans (Choi and He 2015) could be used directly for clinical applications without any preclinical tests. Therefore, $_{ICR}$ESCs have a great deal of potential for significantly reducing the costs and time required for specific clinical applications, such as toxicity evaluation or development of pharmaceuticals and stem cell therapy.

In conclusion, we established ESCs derived from the inner cell mass of blastocysts derived from outbred ICR mice as well as a culture system specific for the established $_{ICR}$ESCs. The established $_{ICR}$ESCs will contribute to studies related to unknown characteristics of ESCs derived from outbred ICR mice and will yield results comparable to human ESCs in preclinical studies alone.

Acknowledgements

This work was supported by the Korea Institute of Planning and Evaluation for Technology in Food, Agriculture, Forestry, and Fisheries (IPET) through Agri-Bioindustry Technology Development Program, funded by the Ministry of Agriculture, Food, and Rural Affairs (MAFRA) (IPET 312060-05 and IPET117042-3).

Disclosure statement

No potential conflict of interest was reported by the author(s).

Funding

This work was supported by the Korea Institute of Planning and Evaluation for Technology in Food, Agriculture, Forestry, and Fisheries (IPET) through Agri-Bioindustry Technology

Development Program, funded by the Ministry of Agriculture, Food, and Rural Affairs (MAFRA) [IPET 312060-05 and IPET117042-3].

ORCID

Na Rae Han http://orcid.org/0000-0001-6279-5150
Song Baek http://orcid.org/0000-0002-5839-1329
Jung Im Yun http://orcid.org/0000-0001-9633-2947
Eunsong Lee http://orcid.org/0000-0001-9654-7788
Seung Tae Lee http://orcid.org/0000-0002-8952-3881

References

Arufe MC, Lu M, Kubo A, Keller G, Davies TF, Lin RY. 2006. Directed differentiation of mouse embryonic stem cells into thyroid follicular cells. Endocrinology. 147:3007.

Chia R, Achilli F, Festing MF, Fisher EM. 2005. The origins and uses of mouse outbred stocks. Nat Genet. 37:1181–1186.

Choi JK, He X. 2015. Improved oocyte isolation and embryonic development of outbred deer mice. Sci Rep. 5:12232.

Choi KM, Jung J, Cho YM, Kim K, Kim MG, Kim J, Kim H, Shin HJ, Kim HD, Chung ST, et al. 2017. Genetic and phenotypic characterization of the novel mouse substrain C57BL/6N Korl with increased body weight. Sci Rep. 7:14217.

Dietrich W, Katz H, Lincoln SE, Shin H, Friedman J, Dracopoli NC, Lander ES. 1992. A genetic map of the mouse suitable for typing intraspecific crosses. Genetics. 131:423–447.

Duncan T, Valenzuela M. 2017. Alzheimer's disease, dementia, and stem cell therapy. Stem Cell Res Ther. 8:111.

Dvash T, Ben-Yosef D, Eiges R. 2006. Human embryonic stem cells as a powerful tool for studying human embryogenesis. Pediatr Res. 60:111–117.

Evans MJ, Kaufman MH. 1981. Establishment in culture of pluripotential cells from mouse embryos. Nature. 292:154–156.

Fox JG, Barthold S, Davisson M, Newcomer CE, Quimby FW, Smith A. 2006. The mouse in biomedical research: normative biology, husbandry, and models (Vol. 3). Amsterdam: Elsevier.

Gerecht-Nir S, Itskovitz-Eldor J. 2004. Human embryonic stem cells: a potential source for cellular therapy. Am J Transplant. 4:51–57.

Hübner K, Fuhrmann G, Christenson LK, Kehler J, Reinbold R, De La Fuente R, Wood J, Strauss JF, Boiani M, Schöler HR. 2003. Derivation of oocytes from mouse embryonic stem cells. Science. 300:1251–1256.

Ilic D, Devito L, Miere C, Codognotto S. 2015. Human embryonic and induced pluripotent stem cells in clinical trials. Br Med Bull. 116:19–27.

Jensen VS, Porsgaard T, Lykkesfeldt J, Hvid H. 2016. Rodent model choice has major impact on variability of standard preclinical readouts associated with diabetes and obesity research. Am J Transl Res. 8:3574–3584.

Kawamata M, Ochiya T. 2010. Generation of genetically modified rats from embryonic stem cells. Proc Natl Acad Sci USA. 107:14223–14228.

Kawase E, Suemori H, Takahashi N, Okazaki K, Hashimoto K, Nakatsuji N. 1994. Strain difference in establishment of mouse embryonic stem (ES) cell lines. Int J Dev Biol. 38:385–390.

Lee KH, Chuang CK, Guo SF, Tu CF. 2012. Simple and efficient derivation of mouse embryonic stem cell lines using differentiation inhibitors or proliferation stimulators. Stem Cells Dev. 21:373–383.

Lee H, Yoon DE, Kim K. 2020. Genome editing methods in animal models. Anim Cells Syst. 24:8–16.

Lou YJ, Liang XG. 2011. Embryonic stem cell application in drug discovery. Acta Pharmacol Sin. 33:152–159.

Martin GR. 1981. Isolation of a pluripotent cell line from early mouse embryos cultured in medium conditioned by teratocarcinoma stem cells. Proc Natl Acad Sci USA. 78:7634–7638.

McKee C, Chaudhry GR. 2017. Advances and challenges in stem cell culture. Colloids Surf B Biointerfaces. 159:62–77.

Meng GL, Tang FC, Shang KG, Xue YF. 2003. Comparison of the method establishing embryonic stem cell lines from five different mouse strains. Journal of Genetics. 30:933–942.

National Research Council. 1999. Microbial and phenotypic definition of rats and mice: proceedings of the 1998 US/Japan conference. Washington, DC: National Academies Press.

Naujok O, Lentes J, Diekmann U, Davenport C, Lenzen S. 2014. Cytotoxicity and activation of the Wnt/beta-catenin pathway in mouse embryonic stem cells treated with four GSK3 inhibitors. BMC Res Notes. 7:273.

Nichols J, Smith A. 2011. The origin and identity of embryonic stem cells. Development. 138:3–8.

Ouyang A, Ng R, Yang ST. 2007. Long-term culturing of undifferentiated embryonic stem cells in conditioned media and three-dimensional fibrous matrices without extracellular matrix coating. Stem Cells. 25:447–454.

Prajumwongs P, Weeranantanapan O, Jaroonwitchawan T, Noisa P. 2016. Human embryonic stem cells: a model for the study of neural development and neurological diseases. Stem Cells Int. 2016:2958210.

Rey A, Manen D, Rizzoli R, Ferrari SL, Caverzasio J. 2007. Evidences for a role of p38 MAP kinase in the stimulation of alkaline phosphatase and matrix mineralization induced by parathyroid hormone in osteoblastic cells. Bone. 41:59–67.

Rocha JL, Eisen EJ, Van Vleck LD, Pomp D. 2004. A large-sample QTL study in mice: II. Body composition. Mamm Genome. 15:100–113.

Ryu J, Park BC, Lee DH. 2019. A proteomic analysis of differentiating dopamine neurons derived from human embryonic stem cells. Anim Cells Syst. 23:219–227.

Schauwecker PE. 2011. The relevance of individual genetic background and its role in animal models of epilepsy. Epilepsy Res. 97:1–11.

Schoonjans L, Kreemers V, Danloy S, Moreadith RW, Laroche Y, Collen D. 2003. Improved generation of germline-competent embryonic stem cell lines from inbred mouse strains. Stem Cells. 21:90–97.

Shin HJ, Cho YM, Shin HJ, Kim HD, Choi KM, Kim MG, Shin HD, Chung MW. 2017. Comparison of commonly used ICR stocks and the characterization of Korl:ICR. Lab Anim Res. 33:8–14.

Štefková K, Procházková J, Pacherník J. 2015. Alkaline phosphatase in stem cells. Stem Cells Int. 2015:628368.

Suzuki A, Guicheux J, Palmer G, Miura Y, Oiso Y, Bonjour JP, Caverzasio J. 2002. Evidence for a role of p38 MAP kinase

in expression of alkaline phosphatase during osteoblastic cell differentiation. Bone. 30:91–98.

Tanimoto Y, Iijima S, Hasegawa Y, Suzuki Y, Daitoku Y, Mizuno S, Ishige T, Kudo T, Takahashi S, Kunita S, et al. 2008. Embryonic stem cells derived from C57BL/6J and C57BL/6N mice. Comp Med. 58:347–352.

Tielens S, Verhasselt B, Liu J, Dhont M, Van Der Elst J, Cornelissen M. 2006. Generation of embryonic stem cell lines from mouse blastocysts developed in vivo and in vitro: relation to Oct-4 expression. Reproduction. 132:59–66.

Trounson A, McDonald C. 2015. Stem cell therapies in clinical trials: progress and challenges. Cell Stem Cell. 17:11–22.

Ukai H, Kiyonari H, Ueda HR. 2017. Production of knock-in mice in a single generation from embryonic stem cells. Nat Protoc. 12:2513–2530.

Wu Y, Liu F, Liu Y, Liu X, Ai Z, Guo Z, Zhang Y. 2015. GSK3 inhibitors CHIR99021 and 6-bromoindirubin-3′-oxime inhibit microRNA maturation in mouse embryonic stem cells. Sci Rep. 5:8666.

Ye J, Bates N, Soteriou D, Grady L, Edmond C, Ross A, Kerby A, Lewis PA, Adeniyi T, Wright R, et al. 2017. High quality clinical grade human embryonic stem cell lines derived from fresh discarded embryos. Stem Cell Res Ther. 8:128.

Yoshiki A, Moriwaki K. 2006. Mouse phenome research: implications of genetic background. ILAR J. 47:94–102.

Zuluaga AF, Salazar BE, Rodriguez CA, Zapata AX, Agudelo M, Vesga O. 2006. Neutropenia induced in outbred mice by a simplified low-dose cyclophosphamide regimen: characterization and applicability to diverse experimental models of infectious diseases. BMC Infect Dis. 6:55.